Journal of Visualized Experiments

Assembly and Characterization of Polyelectrolyte Complex Micelles

--Manuscript Draft--

Article Type:	Invited Methods Article - JoVE Produced Video
Manuscript Number:	JoVE60894R1
Full Title:	Assembly and Characterization of Polyelectrolyte Complex Micelles
Section/Category:	JoVE Bioengineering
Keywords:	Nucleic acid delivery, polyelectrolyte complex, micelle, nanoparticles, phase separation, oligonucleotides
Corresponding Author:	Alexander E. Marras The University of Chicago Chicago, IL UNITED STATES
Corresponding Author's Institution:	The University of Chicago
Corresponding Author E-Mail:	marras@uchicago.edu
Order of Authors:	Alexander E. Marras
	Jeffrey R. Vieregg
	Matthew V. Tirrell
Additional Information:	
Question	**Response**
Please indicate whether this article will be Standard Access or Open Access.	Standard Access (US$2,400)
Please indicate the **city, state/province, and country** where this article will be **filmed**. Please do not use abbreviations.	Chicago, IL

Cover Letter

PRITZKER SCHOOL OF MOLECULAR ENGINEERING

Alexander E. Marras
Postdoctoral Scholar
Pritzker School of Molecular Engineering
5640 South Ellis Ave.
Chicago, IL 60637

O: 773.702.8153
M: 614.565.9362

marras@uchicago.edu

October 13, 2019

Dear Benjamin Werth,

Per our previous correspondence, please find our manuscript titles “Assembly and Characterization of Polyelectrolyte Micelles” attached. We look forward to the next steps with our JoVE manuscript and video. Please do not hesitate to contact me with any questions or concerns.

Sincerely,

Alexander E. Marras

THE UNIVERSITY OF CHICAGO

TITLE:
Assembly and Characterization of Polyelectrolyte Complex Micelles

AUTHORS AND AFFILIATIONS:
Alexander E. Marras[1], Jeffrey R. Vieregg[1], Matthew V. Tirrell[1]

[1]Pritzker School of Molecular Engineering, The University of Chicago, Chicago, IL, USA

Corresponding Author:
Jeffrey R. Vieregg (jvieregg@uchicago.edu)

Email Addresses of Co-authors:
Alexander E. Marras (marras@uchicago.edu)
Matthew V. Tirrell (mtirrell@uchicago.edu)

KEYWORDS:
nucleic acid delivery, polyelectrolyte complex, micelle, nanoparticles, phase separation, oligonucleotides

SUMMARY:
We provide protocols and representative data for designing, assembling, and characterizing polyelectrolyte complex micelles, core-shell nanoparticles formed by polyelectrolytes and charged-hydrophilic neutral block copolymers.

ABSTRACT:
Polyelectrolyte complex micelles (PCMs), core-shell nanoparticles formed by self-assembly of charged polymers in aqueous solution, provide a powerful platform for exploring the physics of polyelectrolyte interactions and also offer a promising solution to the pressing problem of delivering therapeutic oligonucleotides in vivo. Developing predictive structure-property relationships for PCMs has proven difficult, in part due to the presence of strong kinetic traps during nanoparticle self-assembly. This article discusses criteria for choosing polymers for PCM construction and provides protocols based on salt annealing that enable assembly of repeatable, low-polydispersity nanoparticles. We also discuss PCM characterization using light scattering, small-angle X-ray scattering, and electron microscopy.

INTRODUCTION:
When oppositely charged polyelectrolytes are mixed in aqueous solution, entropy gain from release of their counterions causes demixing of the solution into a polymer-rich condensed phase and a polymer-depleted supernatant[1-5], a phenomenon known as polyelectrolyte complexation. If a neutral hydrophilic block is conjugated to one or both of the polyelectrolytes, nanoscale phase separation occurs instead (**Figure 1A**). The resulting self-assembled core-shell nanoparticles are variously referred to as polyelectrolyte complex micelles (PCMs), polyion complex micelles, block ionomer complexes, or coacervate-core micelles by analogy to surfactant

micellization, even though all components of the system are hydrophilic[6,7]. A PCM's ability to encapsulate hydrophilic molecules such as proteins and nucleic acids, as well as the extensive tunability offered by the block copolymer carrier architecture makes them attractive candidates for delivering therapeutic molecules in vivo[8-13].

Delivering therapeutic nucleic acids to cellular targets is a particularly important challenge, and one for which PCMs offer several advantages. Therapeutic nucleic acids (gDNA, mRNA, and siRNA) have immense potential for improving human health, but must overcome numerous biological and physical barriers to realize that potential[14-16]. Bare nucleic acids are degraded by serum and cellular nucleases, are quickly cleared from circulation, and their strong negative charge makes it difficult for them to penetrate cell membranes without assistance. Current approaches for overcoming these barriers include costly chemical modifications to prevent damage from nucleases and/or encapsulation into various lipid nanoparticles assembled via hydrophobic interactions[15,17,18]. While these methods have proven effective for local injections and liver targeting, systemic use presents significant limitations of toxicity, immunogenicity, and limited biodistribution[16]. By contrast, PCMs use the negative charge of nucleic acids to condense them within the phase-separated core, while the neutral corona provides a steric barrier against degradation as well as a platform for incorporating ligands to enhance targeting or internalization[11,19]. In vitro and animal studies have shown that PCMs can effectively deliver various nucleic acid payloads[20-24], but weaknesses in our ability to predict PCM properties such as size, shape, and stability from the properties of the constituent polymers have hindered their wider adoption.

Recent work by our group and others in the field has begun to address this problem by developing structure-property, and in some cases structure-property-function relationships for PCMs formed from nucleic acids and various cationic-neutral polymers[7,25-27]. Two consistent themes that have emerged from these studies are the importance of developing well-controlled, repeatable protocols for PCM assembly and the benefit of using multiple techniques to characterize the resulting nanoparticles. Polyelectrolytes, particularly those with high charge density like nucleic acids, interact with each other very strongly, and appear to readily become kinetically trapped upon mixing, resulting in PCM preparations that are highly sensitive to small variations in procedure and display high polydispersity and poor repeatability from batch to batch. PCMs have also been shown to adopt a wide range of shapes and sizes depending on the atomic-level configurations of their components, and capturing this diversity with any individual characterization technique is very difficult, particularly since some common techniques such as dynamic light scattering (DLS) require assumptions about particle shape for their interpretation.

In this article, we discuss material design and selection for PCMs, with a focus on oligonucleotides and cationic-neutral diblock copolymers. We then describe a salt annealing protocol that uses high salt concentrations followed by slow dialysis to avoid kinetic trapping during PCM assembly. The polyelectrolytes are mixed in high salt conditions where electrostatic attractions are screened, then the salt concentration is slowly lowered to allow the polyelectrolytes to settle into their most energetically favorable configurations, analogous to the slow cooling process of thermal annealing. Using this protocol, we are regularly able to achieve exceptionally low

polydispersity and high repeatability for oligonucleotide PCMs[7,26]. Finally, we describe how four separate measurement techniques can be used to characterize PCMs over a very wide range of length scales, from external morphology to internal structure: DLS, multi-angle light scattering (MALS), small angle X-ray scattering (SAXS), and transmission electron microscopy (TEM). We hope that these protocols will enable more researchers to effectively explore the capabilities of these interesting nanoparticles.

Polymer Selection and Preparation

PCM properties are strongly influenced by the physical and chemical characteristics of the constituent polymers, making polymer selection a critical step in the design process. The most well-characterized block copolymers for nucleic acid PCMs are linear diblocks such as poly(lysine)-poly(ethylene glycol) (pLys-PEG), but PCMs can be formed between polyelectrolytes and a variety of hydrophilic neutral-charged polymers, which can be generated in a high throughput manner[28]. The choice of charged group strongly affects the stability of ion pairing and shape of micelles[26], and PCM size has been shown to increase with the length of the charged block[5,7,26] (**Figure 2**), thus allowing PCM properties to be tuned for the requirements of a desired application. For linear diblocks, we have found that the charged block should have at least 10 charges and be strongly charged at the desired pH. Longer charged blocks may promote PCM formation with oligonucleotides such as siRNA, which are difficult to complex with shorter blocks[21]. We have successfully observed PCM formation with block lengths up to 200, and the literature describes longer polymers. More flexibility is available in the choice of neutral blocks[24], but experience has shown that very short neutral blocks lead to aggregation rather than nanoparticle formation, and that the minimum neutral length increases with charged block length. For pLys-PEG, a PEG MW of at least 3,000–5,000 is required for pLys lengths below ~50, and longer lengths are required as the charged block is increased further. Increased neutral block length results in increased PCM size, particularly shell thickness, due to steric crowding of the neutral polymers.

This manuscript presents a protocol for preparing PCMs from lyophilized high-purity pLys-PEG and oligonucleotides of known quantity, but should be readily adaptable to other systems as well. We have tested it successfully with several charged polypeptides, including polyarginine and polyglutamic acid, as well as several synthetic polyelectrolytes, such as polyacrylic acid and poly(vinylbenzyl trimethylammonium). We also describe preparing PCMs with a stoichiometric ratio of polyelectrolyte charges, but this is easily modified. We find it easiest to work in charge concentration units (c.c.), which also naturally accommodates polymers that are not fully charged. If either polymer is not well-characterized, care should be taken to accurately determine the polymer lengths/masses and ensure that excess salt is not present beyond that needed for charge neutralization by dialysis, for example. The presence of any retained water should also be accounted for when concentrations are calculated. Nucleic acid concentration can be conveniently quantified by absorbance at 260 nm, and the presence or absence of terminal phosphates should be considered when calculating the c.c.

When using oligonucleotides as polyanions, the hybridization state and chemical structure help determine the propensity for self-assembly and the characteristics of the resulting PCM[5,7,26].

Optimizing these, within the requirements for biological efficacy if using PCMs for delivery, will increase the likelihood of forming the desired structures. Helpful tools for analyzing hybridization include MATLAB functions for nucleic acids, NUPACK[29], and IDT OligoAnalyzer. We recommend analyzing a candidate sequence to understand the strength of binding to 1) itself in a hairpin formation; 2) another copy of the same sequence (self-dimer); and 3) to other oligonucleotides present in the system. DNA and RNA melting temperatures for a specific sequence can also be calculated using the nearest-neighbor method[30,31]. Thermal annealing of nucleic acids (step 2.3) denatures any residual secondary structure in the individual nucleotides and promotes equilibrium folding.

PCM Characterization and Analysis

A wide range of techniques are available for characterizing nanoparticles, including static and dynamic light scattering, small angle scattering of electrons or neutrons, and electron microscopy. In this article, we provide protocols for two light scattering techniques, small angle X-ray scattering, and two electron microscopy techniques.

DLS measures the autocorrelation of temporal fluctuations in scattering intensity at one angle from Brownian motion of the sample. Fitting this data can provide hydrodynamic radius and polydispersity for spherical micelles (**Figure 3**). Multiple angle light scattering (MALS) measures the static scattering intensity at many angles. This angular dependence describes the shape of the nanoparticle but is limited to length scales longer than ~50 nm for visible light, which limits its effectiveness for smaller nanoparticles. Both techniques are based on refractive index mismatch and primarily describe the outside dimensions of the nanoparticle.

Small angle X-ray scattering (SAXS) uses X-rays as the scattering probe, and their shorter wavelength allows measurements over a range of ~0.1–100 nm. Fitting the observed scattering intensity vs. angle (conventionally expressed as momentum transfer q) provides information on PCM morphology (i.e., size and shape) and also internal structure. If an absolute intensity calibration is available, and if the scattering intensity can be extrapolated to zero angle, PCM mass and aggregation number can also be estimated[32], making SAXS an extremely versatile and valuable method. Small angle neutron scattering (SANS) is sensitive over a similar range of length scales but is only available at specialized facilities and will not be explicitly discussed in this article[33-35].

Recent years have seen the advent of benchtop SAXS instruments, but we find that synchrotron sources are better suited for PCM characterization, as their higher intensity allows data to be collected much faster for these low-contrast samples. We provide a brief protocol for acquiring PCM SAXS data at Beamline 12-ID-B at the Advanced Photon Source (Argonne National Laboratory, USA) from a user perspective. This protocol should be applicable to most synchrotron sources, but consulting with local staff before proposing an experiment is highly recommended. We also provide a data reduction and analysis protocol using Irena[36], a free set of macros written for Igor Pro. Irena includes a versatile set of form factors for modeling SAXS data and allows for construction of multicomponent models that are capable of describing the complex scattering profile of PCMs (see **Representative Results**, **Figure 4**). Irena also has comprehensive

documentation and tutorials available online. Before attempting the procedures below, we recommend familiarization with these, particularly the tutorial "Modeling of SAXS data with two main scatterer populations".

Radiation damage is a concern for X-ray scattering, but several measures can be employed to minimize it. In particular, we recommend using a flow cell setup with a syringe pump and PCM sample flowing during data acquisition, rather than a sealed capillary. This also greatly simplifies background subtraction. We also suggest taking multiple exposures of the flowing sample rather than one longer one in order to limit the flux that any single volume of sample sees and to allow for comparison of the exposure data to identify any damage.

In contrast to the scattering techniques, which generally require fitting to interpret, transmission electron microscopy (TEM) provides a real space visual image of the nanoparticles by passing an electron beam through the sample and projecting an image on a scintillation screen (**Figure 5**). We present protocols for two TEM techniques in this article. Cryo TEM freezes micelle samples into a thin layer of vitreous ice, preserving structural conformation with minimal foreign substances, optimal for micelles ≤~10-100 nm in radius. Negative stain TEM uses a heavy metal salt (e.g., uranium) to surround the sample after it has been dried on the surface of a grid. The dense stain will scatter more electrons than the sample, adding contrast and producing a negative image of the sample. Cryo TEM is recommended for high-quality images. However, it is more costly, time consuming, and may not provide sufficient contrast. When this is a concern, negative stained samples should be used. Examples of each are shown in **Figure 5**.

Each of these techniques reports on slightly different aspects of the nanoparticles, with different strengths and limitations. Light scattering is readily available, and is often the fastest approach, but has substantial limitations in size and shape resolution. SAXS can provide information over a large range of length scales at reasonably high throughput, but requires specialized equipment to acquire the data, as well as modeling to interpret it. TEM images are straightforward to interpret but can be limited in contrast and are inherently low throughput. Our experience has shown that using multiple techniques for characterization greatly increases the information that can be obtained about PCM properties and simplifies interpretation of data sets obtained from each one alone. For example, SAXS and TEM primarily examine a PCM's dense core, while light scattering reports on the overall dimensions of the nanoparticle. Thus, combining them allows measurement of both core and corona size. TEM's ability to acquire real space images can provide ground truth data to enable selection of appropriate form factors for modeling SAXS data that might otherwise be ambiguous. This article describes protocols for all four techniques, and an example process for using them to characterize an unknown sample is given in the **Discussion** section.

PROTOCOL:

1. Preparation of Materials

1.1. Weigh out lyophilized diblock polymer and add water up to nearly the volume required for a stock solution of 10 mg/mL final concentration. Vortex at maximum speed for 2 min.

1.2. Sonicate for 5 min. Very long diblocks may require additional sonication. The stock solution should appear completely transparent and homogeneous.

1.3. Adjust pH to 7.4 using NaOH or HCl as needed. Add water to the final volume. pLys-PEG solutions are fairly stable but should be refrigerated for longer-term storage and the pH must be checked before use. Lyophilization is preferable to freezing.

1.4. Resuspend lyophilized oligonucleotide(s) at desired stock concentration, typically 2–5 mM molecular concentration for lengths of 50 nt or below. Vortex thoroughly to ensure full dissolution.

1.5. Calculate molar concentrations using molecular weight or length as described in the Introduction.

1.6. Calculate molar charge concentrations (c.c.), where

$$c.c. = (molecular\ concentration) \times (charge)$$

The polyelectrolyte charge is the number of charged monomers, while the nucleic acid charge is the number of bases minus 1, assuming no phosphorylation. Keep in mind that double-stranded DNA will have twice as many charges per molecule compared to single-stranded DNA.

1.7. Create diluted stock at 20 mM c.c. for each polymer.

2. Nucleic Acid Polyelectrolyte Micelle Preparation

2.1. In a 1.5 mL microcentrifuge tube, mix the following to a total volume of 280 µL:

2.1.1. 200 µL of nuclease-free water (ultrapure water for PCMs not containing nucleic acids).

2.1.2. 40 µL of 10x phosphate-buffered saline (PBS, 137 mM sodium chloride, 10 mM phosphate, pH 7.4 when diluted to 1x) or other suitable buffer[37].

2.1.3. 40 µL of 20 mM c.c. oligonucleotide. For double-stranded oligonucleotides, add 20 µL of each strand at 20 mM c.c.

2.2. Incubate the oligonucleotide solution for 5 min at 70 °C. If the calculated melting temperature for the oligonucleotides is higher, the temperature should be increased accordingly. Note that RNA will degrade at elevated temperatures, so this step should not be longer if this or other sensitive components are present.

2.3. Cool for 15 min. Add 40 µL of 20 mM c.c. diblock, then vortex immediately for 20 s at maximum speed. Incubate 5 min at room temperature (RT).

2.4. Perform the salt anneal.

2.4.1. Add 80 µL of 5 M sodium chloride for a final concentration of 1 M NaCl. Vortex for 10 s at maximum speed.

2.4.2. Incubate for 10 min, then load into dialysis cartridges. Note that the listed molecular weight cutoffs are determined for globular proteins and will not be accurate for linear polymers. We find that a 2k MWCO cartridge avoids sample loss and also provides for gradual changes in ionic strength.

2.4.3. Prepare dialysis baths.

2.4.3.1. Calculate the volume of dialysis bath needed:

$$(\text{number of samples}) \times (400\ \mu\text{L/sample}) \times (300\text{x})$$

2.4.3.2. Mix 10x PBS (or other desired buffer), 5 M NaCl, and ultrapure water for a final solution of 1x PBS and 0.5M NaCl, as well as two solutions of 1x PBS.

2.4.4. Load dialysis cartridges.

2.4.4.1. Label cartridges with permanent marker. Soak cartridges in buffer for at least 2 min to hydrate membranes.

2.4.4.2. Remove cap by twisting counterclockwise. Load sample using gel loading pipette tip. Remove excess air by gently squeezing membranes. Replace cap.

2.4.4.3. Put cartridges in the 1x PBS, 0.5 M sodium chloride dialysis bath. Cartridges should float, with both membranes exposed to the bath. Foam floats can be used if needed.

2.4.5. Dialysis

2.4.5.1. Incubate for 24 h stirring slowly with a magnetic stir bar.

2.4.5.2. Move the cartridges to a new bath of 1x PBS or other desired working buffer. Incubate for 24 h, stirring slowly with a magnetic stir bar. Repeat this step.

2.4.6. Recover the sample.

2.4.6.1. Remove the cartridges from the bath. Remove cap and recover sample using a gel loading pipette tip. Note that the recovered volume may be higher than the initial 400 µL due to membrane swelling. Record recovered volume if slight dilution is a concern.

2.4.6.2. Place the sample into a clean 1.5 mL microcentrifuge tube. PCMs prepared in this way should be stable for several months when refrigerated, provided that nuclease contamination has been avoided.

3. Dynamic light scattering

3.1. To ensure dust-free conditions, buffers should be carefully filtered (filtered 3x through a 0.22 µm syringe or vacuum filter) and glassware thoroughly cleaned between samples. It is also important to ensure that the sample has reached thermal equilibrium before conducting the measurement.

3.2. Dilute the PCM sample to 0.2 mM c.c. (10x if using the protocol described above) with the desired working buffer and load into a suitable cuvette. We use a small-volume cuvette, which requires ~200 µL of sample after dilution.

3.3. Set DLS detector position to 90°.

3.4. Adjust the laser power and/or attenuator so the count rate is 100,000–200,000 counts per second (cps), if possible. Count rates as low as 10 kcps can be used, but measurement times may need to be extended to obtain good statistics (step 4.1). Higher count rates should be avoided, as multiple scattering will confound the measurement.

3.5. Acquire data for 1 min. The count rate should be constant over the entire acquisition time; if not, this indicates that some component of the sample or instrument has not yet equilibrated.

3.6. Examine the autocorrelation data. The long-time baseline should be very flat, and the autocorrelation curve should be smooth, with minimal scatter, as shown in **Figure 3A**. Baseline drift indicates lack of equilibrium, and noise in the data can be improved by acquiring more data.

3.7. Fit autocorrelation function.

3.7.1. Use REPES[38,39] to perform regularized inverse Laplace transformation to deliver a distribution of relaxation times and a diffusion coefficient, *D*. This method then calculates hydrodynamic radius, R_h, using the Stokes-Einstein equation:

$$R_h = k_B T / 6\pi\eta D$$

Figure 1B shows a representation of R_h and **Figure 3B** shows the result of REPES.

3.7.2. Alternatively, use other methods, including CONTIN[40,41] (an alternative regularization algorithm), or non-negative least-squares fitting (NNLS). Consistent results from multiple fitting methods is a signature of high-quality data. Note that cumulant analysis (standard on many instruments) gives nonphysical values for multimodal size/length distributions.

4. Multi-angle light scattering

NOTE: Light scattering intensity vs. angle can be measured on a variety of instruments. We have obtained good results using both goniometer-based instruments and multiple-detector instruments, run in batch mode.

4.1. Adjust the PCM concentration and illumination intensity to provide sufficient signal/noise vs. a buffer-only sample at all angles without saturating any detector. The latter can be tested by preparing samples at various dilution factors and checking for linearity of intensity vs. concentration (assuming minimal interaction between the PCMs).

4.2. Record the light scattering rate from 15° to 135° for 1 min per angle. If the sample and instrument are properly equilibrated, the scattering rate will be constant over the measurement time.

4.3. Plot the normalized scattering rate, $I\sin(\theta)$, vs. q, where I is the scattering rate. q is the scattering vector (photon momentum transfer) as defined by

$$q = 4\pi\eta \sin(\theta/2)/\lambda$$

where η = the solvent refractive index, θ = the measurement angle, and λ = the wavelength of the light source. **Figure 4** shows a plot of MALS scattering intensity.

5. Small angle X-ray scattering

5.1. Data acquisition

5.1.1. Prepare PCM samples as described above at 2 mM charge concentration for oligonucleotide PCMs for ample scattering above background. For PCMs lacking heavy atoms (e.g., phosphorus in nucleic acids), higher concentrations may be required. Scattering length densities can be estimated using calculators such as SASSIE[42].

5.1.2. In order to minimize radiation damage by scavenging free radicals, add glycerol from a concentrated (e.g., 50%) stock solution so that the micelle solution contains 1% (v/v) glycerol. Note that neat glycerol is highly viscous and difficult to accurately measure. Diluting with water or buffer is highly recommended.

5.1.3. Prepare a large volume of working buffer with 1% glycerol for use as a background monitor.

5.1.4. Prepare the beamline specific flow cell apparatus and calibrate detector. The protocol uses a 3 mm diameter quartz capillary connected to a computer-controlled syringe pump with a small diameter, and minimal length polyethylene tubing. A minimum volume of ~140 µL per sample is needed with this setup.

5.1.5. Determine sample exposure parameters. The optimum exposure will vary based on beam intensity, detector sensitivity, and the concentration, scattering strength, and damage susceptibility of the sample, but the goal is to expose the sample to the minimal flux required to obtain sufficient scattering intensity over the *q* range of interest.

5.1.6. For oligonucleotide/pLys-PEG PCMs, 30x 0.2 s exposures at a 1 Hz repetition rate produce good data quality with little perceptible damage. For new samples, the following procedure may be helpful:

5.1.6.1. Prepare PCM samples over a range of concentrations (e.g., 10–10,000 µM c.c.).

5.1.6.2. Starting at an intermediate concentration, alternate PCM and buffer-only samples with varying exposure times. See below for data acquisition and reduction procedure. Sample signal should have good statistics (small statistical error, or smooth variation across *q*). If the statistics are poor, the exposure time may be increased.

5.1.6.3. Sample signal should also be clearly distinguishable from background over the *q* range of interest. Compute and plot the (signal–background)/background ratio vs. *q* to determine signal/background ratio. If the signal/background ratio is low, sample concentration should be increased.

5.1.6.4. Verify that the scattering intensity (normalized to concentration) is independent of sample concentration by acquiring data at higher and lower concentrations, scaling exposure time if needed. Interparticle interactions (the most likely cause of concentration dependence) will be most pronounced in the low *q* range.

5.1.7. Acquire data for PCM samples and background (i.e., buffer with glycerol).

5.1.7.1. Trigger the syringe pump to move the sample through the capillary. Either bidirectional or once-through motion is acceptable, but care should be taken to isolate each sample (e.g., by inserting an air bubble between samples). Samples may be recovered and can be reused if no radiation damage is seen.

5.1.7.2. Once flow has started, trigger the X-ray exposure and data acquisition program described above. Care should be taken that the beam exposure ends before fluid flow does.

5.1.8. After each sample, perform azimuthal averaging and plot the 1D profiles (i.e., intensity vs. *q*) for each exposure together. They should be identical within statistical error. Changing signal over time can indicate radiation damage.

5.1.8.1. Isolated anomalous profiles may indicate the presence of microbubbles. If bubbles are observed frequently, decreasing the flow rate may help.

5.1.9. Average the 1D scattering profiles.

5.1.10. Acquire data for buffer-only samples frequently (once per every 4–5 PCM samples) and compare these over time. Increased signal from buffer-only samples indicates that the capillary may be contaminated with radiation-damaged sample.

5.1.10.1. When contamination is noticed, wash the capillary with bleach, and consider reducing exposure time if possible.

5.2. Data reduction and analysis using Irena

5.2.1. Import micelle and background ASCII data sets (**SAS/Data import & export/Import ASCII SAS data**).

5.2.2. Subtract background scattering from sample data. Typically, the highest q values (e.g. q > 0.5) show incoherent scattering from the solvent dominating the signal. Scaling the background data to match the sample data over this q range removes any variation due to beam intensity variation and sample concentration.

5.2.2.1. Plot the sample and background together on a log-log scale. Verify flat intensity at high q (**SAS/Data Manipulation/Data Manipulation I**). Compute the sample/background ratio (**Data1/Data 2**), plot on a linear-log scale, and verify the high-q asymptote.

5.2.2.2. Compute the average (sample/background) ratio over this q range (use a custom macro or copy/paste into a spreadsheet from the data browser).

5.2.2.3. Using the **Data Manipulation** macro, scale the background (e.g., **Modify Data 2**) using the ratio computed above and plot the ratio of background-subtracted signal to background vs. q (**[Data1-Data2]/Data2**), verifying that it now asymptotes to zero at high q. Record this ratio; it should be <1–2% away from 1.0 for each sample.

5.2.2.4. Plot the background-subtracted signal (**Data1-Data2**) vs. q and save the data with a new name. Do not overwrite the original data.

5.2.2.5. If high-q data is not available, use a scaling factor of 1 for background subtraction, but be aware that inaccuracies may be introduced in q ranges where the signal/background ratio is small.

5.2.3. Open the **Modeling** macro, (**SAS/Modeling**), then load and plot the background-subtracted data (**Data cntrls/Add data**). Do not scale in this macro.

5.2.4. First, find an approximate model for the external surface of the PCM (micelle size/shape):

5.2.4.1. In **Data cntrls**, select low to moderate *q* range (e.g., ~0.003Å^{-1} < *q* < ~0.1Å^{-1}). If oscillations are visible, include them.

5.2.4.2. Choose a form factor appropriate for the data. The slope at low *q* is indicative of nanoparticle shape, which can also be verified through TEM and/or MALS. Use Schulz-Zimm spheroid (q^0), cylinder (q^{-1}), or flexible cylinder (q^{-2}) models. Irena provides tools for fitting power laws (**SAS/Support Tools for plots and tables**).

5.2.4.3. In **Model cntrls**, select the first scattering population (**1P**) and make sure it is the only one in use (Select the **Use?** checkbox).

5.2.4.4. Select **Size dist.** for **Model** and choose the desired **Distribution type** and **Form Factor**. Set initial parameters for the search by entering values in the **Scale**, **Mean Size**, and **Width** fields and click **Calculate Model** to draw the resulting form factor.

5.2.4.5. Once reasonable parameters have been found, click **Fit Model** to perform a nonlinear least-squares fit to the data. The **Size distribution** model gives mean radius and width.

To calculate polydispersity (PDI) use

$$PDI = (stdev/radius)^2 = [(width^2)/4]/(radius^2)$$

As with any nonlinear fitting procedure, it may be necessary to adjust the data range (*q* region) and starting parameters in order to obtain a stable, physically reasonable fit.

5.2.4.6. Once a reasonable fit is obtained, save it (**Store in Notebook/Store in Folder**).

NOTE: The individual polymers within the PCM core also scatter X-rays, and this can be captured by a power law model (e.g., q^{-2} for ideal chains, $q^{-5/3}$ for swollen chains, etc.). Irena implements this through a Beaucage model[43]:

$$I(q) = Gexp(-q^2{R_g}^2/3) + B\{[\mathrm{erf}(qR_g/6^{1/2})]^3/q\}^P$$

where P is the power law and G and B are prefactors.

5.2.4.7. Adjust the data controls to cover the entire *q* range and replot the model (**Calculate Model**). Typically, excess scattering will be observed in the moderate to high *q* range (e.g., *q* > ~0.1Å^{-1}).

5.2.4.8. Use the data controls to select the *q* range where excess scattering (>10x the form factor model) is observed.

5.2.4.9. Add a second scattering population (**2P**) and make sure it is the only one in use (deselect **Use?** for **1P**).

5.2.4.10. Select Unified level for the model. B and P are the relevant parameters. Use the plotting support tools or the **Fit P/B between csrs** macro to obtain an initial guess for these parameters, and adjust the Guinier factors G and R_g to ensure that the model does not predict excessive scattering at low *q*.

5.2.4.11. As for the form factor, perform a nonlinear fit and record the parameters and model.

5.2.5. If a diffraction peak is present, as in **Figure 4**, add a third model for a diffraction peak in the *q* range of interest (*q* = ~0.22 $Å^{-1}$ in this case).

5.2.6. Once approximate fit values are obtained for the individual scattering populations, turn on all three together (select **Use?** for each) and optimize the combined fit.

5.2.7. Check that each value remains physically reasonable. The result of this procedure should be a composite model that describes the SAXS data well over a large range of size scales, as illustrated in **Figure 4**. Save the fit.

6. Transmission Electron Microscopy (TEM)

6.1. Cryo TEM

6.1.1. Select the grid. We recommend holey carbon support film on a standard TEM grid or lacey carbon as an alternative. In either case, the holes between the carbon will provide an imaging area of pure vitreous ice and sample and no film.

6.1.2. Place the grid carbon side up in a glow discharging apparatus on a clean glass slide. Wrapping the slide in laboratory film can help with grid handling. Avoid touching the center of the grid with tweezers and always pinch near the edge of the grid.

6.1.3. Expose the grid for 30 s.

6.1.4. Prepare a vitrification robot for sample deposition.

6.1.4.1. Set to 100% humidity and RT and add blotting paper. Prepare liquid ethane and liquid nitrogen baths at the base of the robot. See online tutorials and videos for additional help with vitrification robot preparation and use.

6.1.5. Dilute sample 5x.

6.1.6. Using the negative action tweezers provided with the vitrification robot, pick up a grid, then attach the tweezers to the robot and move the tweezers into the chamber.

6.1.7. While in the robot, add 4 µL of the sample to the carbon side of the grid using a pipette through the hole in the side of the machine.

6.1.8. Incubate for 4 min.

6.1.9. Using the robot, blot 3–5 s with filter paper.

6.1.10. The vitrification robot will plunge the grid into liquid ethane.

6.1.11. Remove the tweezers and move the grid to liquid nitrogen and into a storage container, which should also be under liquid nitrogen. This process fixes the sample into a thin layer of vitreous ice. Minimize the time the grid spends out of the liquid ethane or liquid nitrogen during this step.

6.1.12. Cool the cryo sample holder using liquid nitrogen. Keep a Dewar reservoir full.

6.1.13. When ready to image, load the grid onto the cryo sample holder. Keep the sample under liquid nitrogen or briefly in the extremely cold nitrogen steam just above the liquid surface.

6.1.14. Image the grid at 120 kV between 75kx and 150kx in thin and thick ice, because different sized micelles may prefer a certain ice thickness.

6.1.14.1. Limit beam exposure to avoid melting ice and damaging the sample. Do not focus directly where planning to image; focus nearby. Only expose the area of interest while capturing an image.

6.1.14.2. Be sure to differentiate liquid ethane drops from the sample when viewing images (see **Figure 5**).

6.2. Conventional TEM using negative staining

6.2.1. Prepare the stain.

6.2.1.1. Boil ~10 mL of ultrapure water. Weigh out 0.1 g uranyl formate (UFo) into a 15 mL conical tube.

6.2.1.2. Add 5 mL of the hot water to the UFo powder for a 2% solution. Close tightly and wrap in aluminum foil to block light. A 1% uranyl acetate stain is also commonly used.

6.2.1.3. Vortex or shake vigorously for 5 min. Fastening the tube to the vortexer will help. Filter through a 0.2 µm syringe filter into a clean conical tube.

6.2.1.4. Let cool 10 min to RT. Add 25 µL of 5M NaOH and vortex immediately for 2 min.

6.2.1.4.1. Alternatively, freeze 200 µL aliquots of 2% UFo. When ready for use, thaw an aliquot, add 1 µL of 5 M NaOH, and vortex for 2 min.

6.2.1.5. Keep stain wrapped in foil or away from light.

6.2.2. Dilute sample 10x in 1x PBS (or desired buffer).

6.2.3. Select grid. Carbon support film on copper grids are best. The darker, shinier side of the grid is the carbon-coated side where the sample will be deposited and stained.

6.2.4. Place the grid carbon side up in a glow discharging apparatus on a clean glass slide. See step 6.1.2.

6.2.5. Expose the grid for 30 s.

6.2.6. Pick up the grid with the carbon side still facing up and hold with negative action tweezers by the edge of the grid to prevent tearing the imaging area in the center. Set down the tweezers with the grid still held carbon side up.

6.2.7. Apply a 4 µL droplet of sample to the top (carbon side) of the grid with a pipette.

6.2.8. Incubate 4 min.

6.2.9. With ~1 min left, pipette a 10 µL and a 20 µL drop of UFo solution onto a piece of clean laboratory film.

6.2.10. Use filter paper to wick the sample from the edge of the grid (perpendicular contact) to avoid any contact with the imaging surface.

6.2.11. Using the tweezers (still holding the grid), immediately place the sample side of the grid down on the 10 µL UFo droplet, then immediately wick off the liquid (wash step). It is important not to let the grid dry, so do not stop in between steps.

6.2.12. In a similar manner, apply the 20 µL UFo droplet to the grid. Hold the grid on the UFo for 40 s. Wick the liquid off and let the grid dry.

6.2.13. Image the dry grid at 120 kV between 20,000x and 100,000x.

6.2.14. Be sure to properly dispose of all UFo-contaminated materials using the institution's safety service for radioactive waste.

6.2.15. When necessary, brightness/contrast enhancement and a median filter can be applied to TEM images in ImageJ to reduce background noise. Post processing should be done uniformly, only for images that are not utilized for quantitative measurements such as intensity, and should always be reported.

REPRESENTATIVE RESULTS:

In order to illustrate the characterization methods described above, we show typical results for PCMs assembled from oligonucleotides and block copolymers of various lengths and chemistries (**Figure 1**). **Figure 2** provides an example of how PCM core size (as determined from SAXS and TEM, **Figure 4** and **Figure 5**) varied with charged block length. **Figure 3** shows DLS data and fitting results for spherical PCMs formed from relatively long block copolymers and short single-stranded oligonucleotides. **Figure 4** illustrates how complex SAXS intensity spectra could be accurately fit by combining models for the multiple spatial correlations that were present (external surface, intra-core scattering, inter-helix ordering), and how MALS could be used to extend scattering measurements to longer length scales. Finally, **Figure 5** shows representative electron microscopy data for PCMs of varying morphology.

Figure 1: Assembly and characterization of nucleic acid PCMs. (**A**) Anionic polymers, such as oligonucleotides, formed phase-separated complexes with cationic regions of diblock copolymers. The presence of a hydrophilic neutral block (gray) resulted in formation of stable PCM nanoparticles. (**B**) PCMs were core-shell nanoparticles with multiple parameters to characterize. The overall size (hydrodynamic radius, R_h) could be determined using DLS, the core radius (R_c) could be found using SAXS and TEM, corona size could be calculated as R_h-R_c, and morphology could be determined over multiple length scales by combining SAXS, MALS, and TEM.

Figure 2: Micelle size dependence. Micelle core size was primarily determined by the length of the charged block of the block copolymer, and largely independent of the length of the homopolymer[7,26]. This allows for control of PCM size by choice of block polymer. The data shown here are for pLys-PEG with 88 nt/bp DNA and have been previously reported[26].

Figure 3: Dynamic light scattering. (**A**) Autocorrelation function (arbitrary units) for 10 nt single-stranded DNA + pLys(100)-PEG(10k) PCM. (**B**) Hydrodynamic radius distribution (histogram) from REPES fit. The autocorrelation function decayed to a flat value with a single time scale, resulting in a single size peak in the REPES size distribution.

Figure 4: Representative SAXS and MALS data and fit for a cylindrical micelle. SAXS data (gray circles) are shown for PCMs assembled from pLys(50)-PEG(5k) and 88 bp double-stranded DNA. At low q ($< 10^{-2}$ Å^{-1}), the intensity showed an approximately q^{-2} dependence on momentum transfer, implying a flexible cylinder shape (worm-like micelle). MALS data (open black circles) show the same dependence, indicating that the micelles were at least several micrometers in

length (corroborated by TEM imaging, **Figure 5C**,**D**). Spheroidal micelles would show a flat dependence (q^0) of intensity on *q* in this range. The colored lines illustrate the multicomponent fitting procedure for PCM SAXS data described in section 5. Scattering at low *q* (large distance scales) was dominated by the external surface of the PCM, and fit well by a flexible cylinder model (red). At higher *q* values (smaller length scale), scattering was dominated by the individual polymers inside the PCM core, fit here by a power law (green) with low *q* cutoff. We also observed parallel packing of double-stranded DNA helices within the PCM core, resulting in a quasi-Bragg diffraction peak (blue). The black dashed line shows that combining these models accurately described the SAXS data, and the addition of light scattering data (open circles) extended the size range over nearly four orders of magnitude. Fitting results gave a PCM population with mean radius = 11.0 nm and PDI = 0.03, power law at high *q* = 1.81 and the diffraction peak represents inter-helix spacing of 2.71 nm. SAXS data have been previously reported[26] and are publicly available[44].

Figure 5: TEM images of nucleic acid PCMs. (**A**–**B**) Cryo TEM of 22 nt single-stranded DNA + pLys(50)-PEG(5k) PCMs, showing predominantly spherical morphology. Blue arrows indicate liquid ethane droplets, not to be confused with the PCMs (textured spheroidal objects). (**A**) is slightly under-focused, adding slight contrast while preserving resolution. (**B**) is substantially under-focused, adding more contrast but sacrificing clarity. Brightness and contrast adjustments and a two pixel median filter were applied to both images. (**C**-**D**) Negative stained TEM of 88 bp double-stranded DNA + pLys(50)-PEG(5k) PCMs, which are long flexible cylinders. In both cases, core radii from TEM were consistent with the values obtained from fitting SAXS data.

DISCUSSION:

As mentioned above, the protocols presented here are written with a focus on oligonucleotides as the polyanion component and pLys-PEG as the cationic-neutral block copolymer, but we have tested them with a variety of polymers, such as polyacrylic acid, polyglutamate, and PEG-poly(vinylbenzyl trimethylammonium), and believe they will be generally applicable for most polyelectrolyte pairs. One parameter that may need to be optimized is the salt concentration used for annealing, because it should be high enough that PCMs do not form at the beginning of the anneal. This can be checked experimentally by DLS, or by comparison to observation of phase separation with the polyelectrolytes alone (no neutral block). Thermal annealing can be used if salt annealing is undesirable, though the resulting polydispersities are larger[7]. The concentrations used for characterization also may need to be optimized, because larger nanoparticles scatter more light than small ones, and nucleic acids are more efficient at scattering X-rays than many other polymers due to the presence of electron-dense phosphorus atoms in the backbone. It may also be necessary to more closely control the pH of the buffer if either polyelectrolyte has a pKa close to the working condition.

In this article we present protocols for two light scattering techniques (i.e., multi-angle/static light scattering and dynamic light scattering), as well as small angle X-ray scattering, and both cryo and conventional negative stain transmission electron microscopy, with representative data for each. Not all techniques are necessary for all scenarios, and others are available as well, raising the question of which should be employed when. Ample review literature exists on this

subject[45,46], but we suggest the following when characterizing a new PCM or similar nanoparticle. Begin by checking for aggregation, both by visual inspection for turbidity and by optical microscopy. If no aggregation is observed, the next step is to determine whether any nanoparticles exist. DLS is a quick way to determine this because PCMs scatter light vigorously, and weak or nonexistent light scattering is a strong indicator of poor nanoparticle formation. While DLS can confirm the presence of nanoparticles, it is difficult to determine their size and shape without reference to other data, as most analysis methods rely on the Stokes-Einstein relation, which assumes spherical particles. MALS can confirm spherical shapes (flat normalized intensity vs. angle) but may not be able to determine the shape of nonspherical particles unless the size distribution is both narrow and happens to fall in the correct range for resolution. As a result, we recommend performing TEM, SAXS, or both on any PCM sample in order to fully characterize its properties.

ACKNOWLEDGEMENTS:

We thank Phil Griffin and Tera Lavoie of the Soft Matter Characterization Facility and Advanced Electron Microscopy Facility, respectively, at The University of Chicago. We also thank Xiaobing Zuo and Soenke Seifert of the Advanced Photon Source at Argonne National Laboratory and NIST Center for Hierarchical Materials Design (CHiMaD) for support. We thank Jeff Ting and Michael Lueckheide for their contributions to this work.

REFERENCES:

1. Spruijt, E., Westphal, A. H., Borst, J. W., Cohen Stuart, M. A., van der Gucht, J. Binodal compositions of polyelectrolyte complexes. *Macromolecules.* **43** (15), 6476–6484 (2010).
2. van der Gucht, J., Spruijt, E., Lemmers, M., Cohen Stuart, M. A. Polyelectrolyte complexes: bulk phases and colloidal systems. *Journal of Colloid and Interface Science.* **361** (2), 407–422 (2011).
3. Priftis, D., Laugel, N., Tirrell, M. Thermodynamic characterization of polypeptide complex coacervation. *Langmuir.* **28** (45), 15947–15957 (2012).
4. Fu, J., Schlenoff, J. B. Driving Forces for Oppositely Charged Polyion Association in Aqueous Solutions: Enthalpic, Entropic, but Not Electrostatic. *Journal of the American Chemical Society.* **138** (3), 980–990 (2016).
5. Vieregg, J. R. et al. Oligonucleotide-Peptide Complexes: Phase Control by Hybridization. *Journal of the American Chemical Society.* **140** (5), 1632–1638 (2018).
6. Voets, I. K., de Keizer, A., Cohen Stuart, M. A. Complex coacervate core micelles. *Advances in Colloid and Interface Science.* **147–148**, 300–318 (2009).
7. Lueckheide, M., Vieregg, J. R., Bologna, A. J., Leon, L., Tirrell, M. V. Structure-Property Relationships of Oligonucleotide Polyelectrolyte Complex Micelles. *Nano Letters.* **18** (11), 7111–7117 (2018).
8. De Kruif, C. G., Weinbreck, F., de Vries, R. Complex coacervation of proteins and anionic polysaccharides. *Current Opinion in Colloid & Interface Science.* **9** (5), 340–349 (2004).
9. Vieregg, J. R., Tang, T. Y. D. Polynucleotides in cellular mimics: Coacervates and lipid vesicles. *Current Opinion in Colloid & Interface Science.* **26**, 50–57 (2016).
10. Marciel, A. B., Chung, E. J., Brettmann, B. K., Leon, L. Bulk and nanoscale polypeptide based polyelectrolyte complexes. *Advances in Colloid and Interface Science.* **239**, 187–198 (2017).

11. Cabral, H., Miyata, K., Osada, K., Kataoka, K. Block Copolymer Micelles in Nanomedicine Applications. *Chemical Reviews.* **118** (14), 6844–6892 (2018).
12. Tan, Z. et al. Block Polymer Micelles Enable CRISPR/Cas9 Ribonucleoprotein Delivery: Physicochemical Properties Affect Packaging Mechanisms and Gene Editing Efficiency. *Macromolecules.* **52** (21), 8197–8206 (2019).
13. Horn, J. M., Kapelner, R. A., Obermeyer, A. C. Macro- and Microphase Separated Protein-Polyelectrolyte Complexes: Design Parameters and Current Progress. *Polymers.* **11** (4), E578 (2019).
14. Juliano, R. L. The delivery of therapeutic oligonucleotides. *Nucleic Acids Research.* **44** (14), 6518–6548 (2016).
15. Kanasty, R., Dorkin, J. R., Vegas, A., Anderson, D. Delivery materials for siRNA therapeutics. *Nature Materials.* **12** (11), 967–977 (2013).
16. Lorenzer, C., Dirin, M., Winkler, A. M., Baumann, V., Winkler, J. Going beyond the liver: progress and challenges of targeted delivery of siRNA therapeutics. *Journal of Controlled Release.* **203**, 1–15 (2015).
17. Allen, T. M., Cullis, P. R. Liposomal drug delivery systems: from concept to clinical applications. *Advanced Drug Delivery Reviews.* **65** (1), 36–48 (2013).
18. Li, W., Szoka, F. C., Jr. Lipid-based nanoparticles for nucleic acid delivery. *Pharmaceutical Research.* **24** (3), 438–449 (2007).
19. Miyata, K., Nishiyama, N., Kataoka, K. Rational design of smart supramolecular assemblies for gene delivery: chemical challenges in the creation of artificial viruses. *Chemical Society Reviews.* **41** (7), 2562–2574 (2012).
20. Oishi, M., Nagasaki, Y., Itaka, K., Nishiyama, N., Kataoka, K. Lactosylated poly(ethylene glycol)-siRNA conjugate through acid-labile ss-thiopropionate linkage to construct pH-sensitive polyion complex micelles achieving enhanced gene silencing in hepatoma cells. *Journal of the American Chemical Society.* **127** (6), 1624–1625 (2005).
21. Christie, R. J. et al. Targeted polymeric micelles for siRNA treatment of experimental cancer by intravenous injection. *ACS Nano.* **6** (6), 5174–5189 (2012).
22. Kuo, C. H. et al. Inhibition of atherosclerosis-promoting microRNAs via targeted polyelectrolyte complex micelles. *Journal of Materials Chemistry B.* **2** (46), 8142–8153 (2014).
23. Ge, Z. et al. Targeted gene delivery by polyplex micelles with crowded PEG palisade and cRGD moiety for systemic treatment of pancreatic tumors. *Biomaterials.* **35** (10), 3416–3426 (2014).
24. Van Bruggen, C., Hexum, J. K., Tan, Z., Dalai, R. J., Reineke, T. M. Nonviral Gene Delivery with Cationic Glycopolymers. *Accounts of Chemical Research.* **52** (5), 1347–1358 (2019).
25. Hayashi, K. et al. Influence of RNA Strand Rigidity on Polyion Complex Formation with Block Catiomers. *Macromolecular Rapid Communications.* **37** (6), 486–493 (2016).
26. Marras, A. E., Vieregg, J. R., Ting, J. M., Rubien, J. D., Tirrell, M. V. Polyelectrolyte Complexation of Oligonucleotides by Charged Hydrophobic-Neutral Hydrophilic Block Copolymers. *Polymers.* **11** (1), 83 (2019).
27. Phillips, H. R. et al. Glycopolycation–DNA Polyplex Formulation N/P Ratio Affects Stability, Hemocompatibility, and in Vivo Biodistribution. *Biomacromolecules.* **20** (4), 1530–1544 (2019).
28. Ting, J. M., Wu, H., Herzog-Arbeitman, A., Srivastava, S., Tirrell, M. V. Synthesis and Assembly of Designer Styrenic Diblock Polyelectrolytes. *ACS Macro Letters.* **7** (6), 726–733 (2018).

29. Zadeh, J. N. et al. NUPACK: Analysis and design of nucleic acid systems. *Journal of Computational Chemistry.* **32** (1), 170–173 (2011).
30. Santa Lucia, J., Jr. A unified view of polymer, dumbbell, and oligonucleotide DNA nearest-neighbor thermodynamics. *Proceedings of the National Academy of Sciences of the United States of America.* **95** (4), 1460–1465 (1998).
31. Xia, T. et al. Thermodynamic parameters for an expanded nearest-neighbor model for formation of RNA duplexes with Watson-Crick base pairs. *Biochemistry.* **37** (42), 14719–14735 (1998).
32. Orthaber, D., Bergmann, A., Glatter, O. SAXS experiments on absolute scale with Kratky systems using water as a secondary standard. *Journal of Applied Crystallography.* **33** (2), 218–225 (2000).
33. Srivastava, S. et al. Gel phase formation in dilute triblock copolyelectrolyte complexes. *Nature Communications.* **8**, 14131 (2017).
34. Lindhoud, S. et al. Salt-induced disintegration of lysozyme-containing polyelectrolyte complex micelles. *Langmuir.* **25** (19), 11425–11430 (2009).
35. Lindhoud, S., de Vries, R., Schweins, R., Stuart, M. A. C., Norde, W. Salt-induced release of lipase from polyelectrolyte complex micelles. *Soft Matter.* **5** (1), 242–250 (2009).
36. Ilavsky, J., Jemian, P. R. Irena: tool suite for modeling and analysis of small-angle scattering. *Journal of Applied Crystallography.* **42** (2), 347–353 (2009).
37. Sambrook, J., Fritsch, E. F., Maniatis, T. *Molecular Cloning: a Laboratory Manual*. (Cold Spring Harbor Laboratory Press, 1989).
38. Jakeš, J. Regularized positive exponential sum (REPES) program-A way of inverting laplace transform data obtained by dynamic light scattering. *Collection of Czechoslovak Chemical Communications.* **60** (11), 1781–1797 (1995).
39. Schillen, K., Brown, W., Johnsen, R. M. Micellar Sphere-to-Rod Transition in an Aqueous Triblock Copolymer System - a Dynamic Light-Scattering Study of Translational and Rotational Diffusion. *Macromolecules.* **27** (17), 4825–4832 (1994).
40. Provencher, S. W. Contin - a General-Purpose Constrained Regularization Program for Inverting Noisy Linear Algebraic and Integral-Equations. *Computer Physics Communications.* **27** (3), 229–242 (1982).
41. Provencher, S. W. A Constrained Regularization Method for Inverting Data Represented by Linear Algebraic or Integral-Equations. *Computer Physics Communications.* **27** (3), 213–227 (1982).
42. Sarachan, K. L., Curtis, J. E., Krueger, S. Small-angle scattering contrast calculator for protein and nucleic acid complexes in solution. *Journal of Applied Crystallography.* **46** (6), 1889–1893 (2013).
43. Beaucage, G. Approximations leading to a unified exponential power-law approach to small-angle scattering. *Journal of Applied Crystallography.* **28** (6), 717–728 (1995).
44. Marras, A. E., Vieregg, J. R., Ting, J. M., Rubien, J. D., Tirrell, M. V. 10.18126/M2QW8R (Materials Data Facility, 2018).
45. Modena, M. M., Rühle, B., Burg, T. P., Wuttke, S. Nanoparticle Characterization: What to Measure? *Advanced Materials.* 1901556 (2019).

871 46. Mourdikoudis, S., Pallares, R. M., Thanh, N. T. K. Characterization techniques for
872 nanoparticles: comparison and complementarity upon studying nanoparticle properties.
873 *Nanoscale.* **10** (27), 12871–12934 (2018).
874

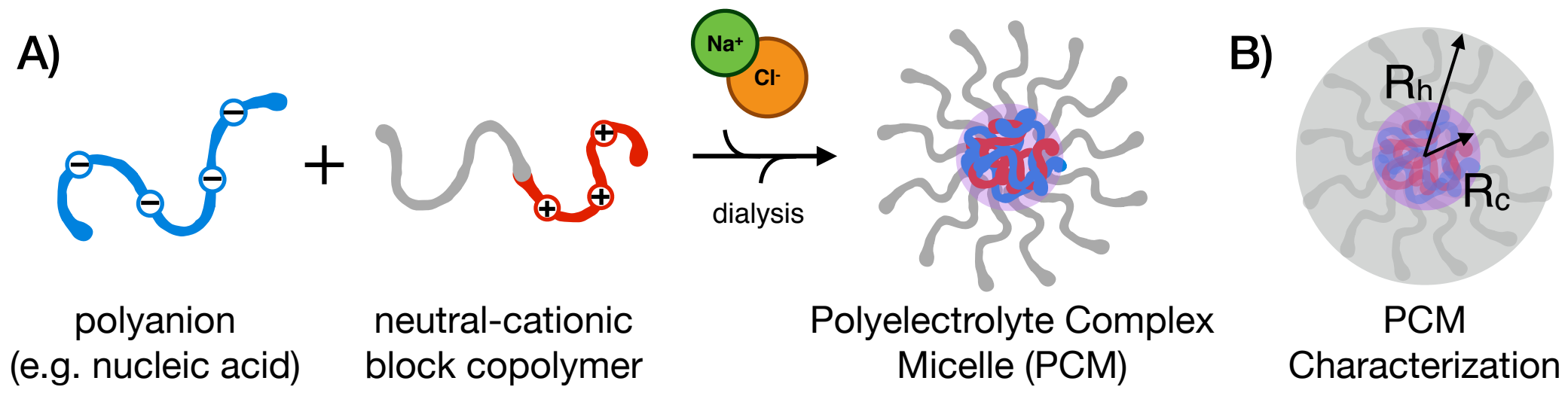
A)
Na+
Cl-
dialysis
B)
Rh
Rc
polyanion
(e.g. nucleic acid)
neutral-cationic
block copolymer
Polyelectrolyte Complex
Micelle (PCM)
PCM
Characterization

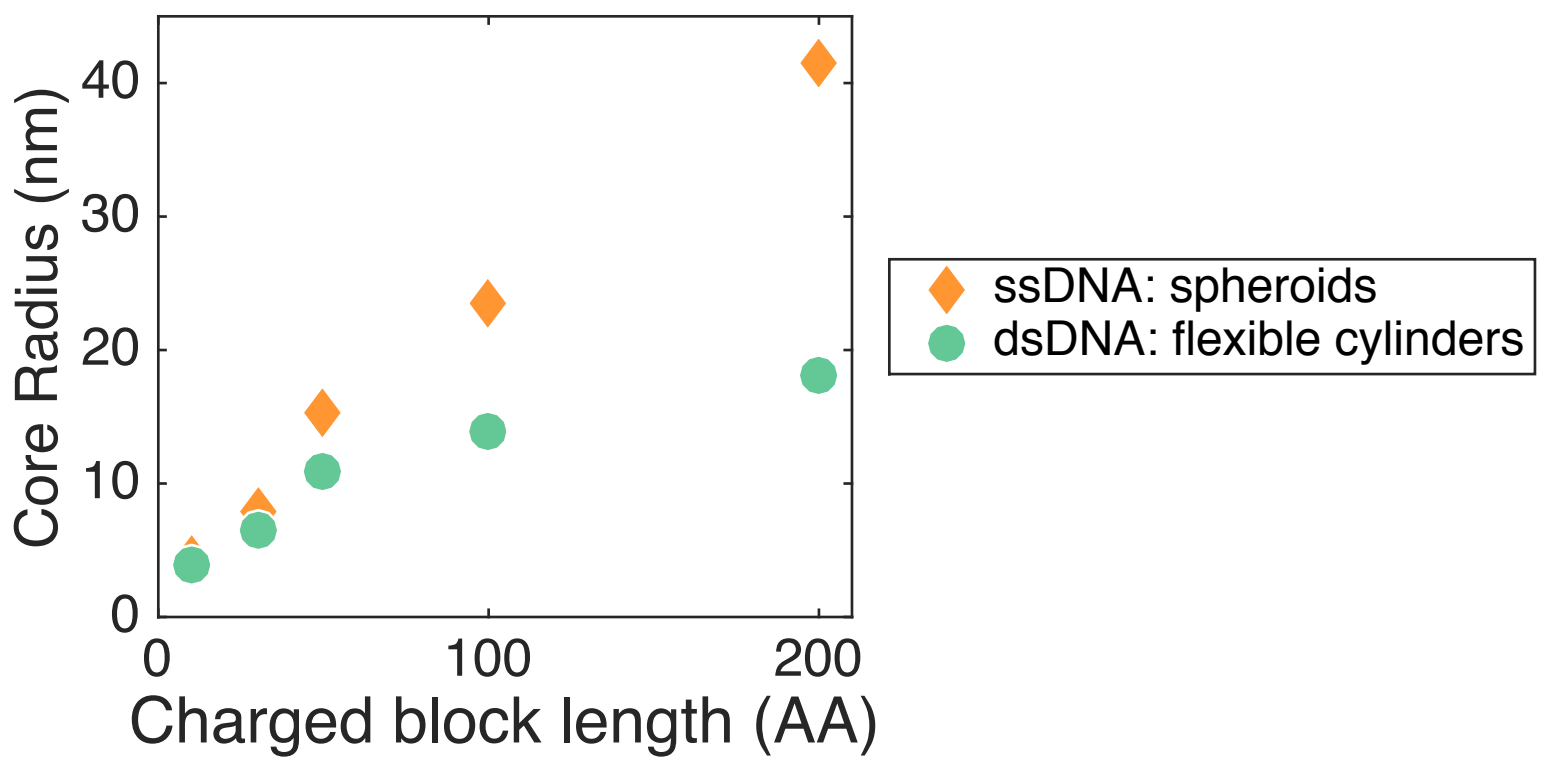
Core Radius (nm)
0
10
20
30
40
0
100
200
Charged block length (AA)
ssDNA: spheroids
dsDNA: flexible cylinders

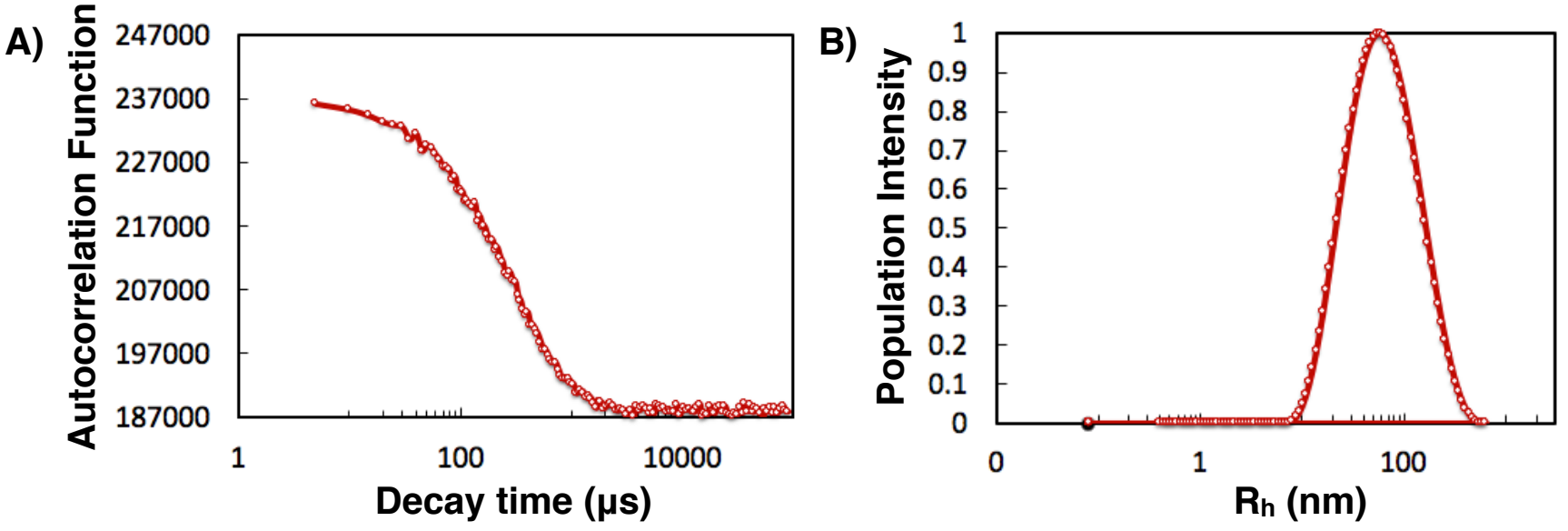
A)
Autocorrelation Function
247000
237000
227000
217000
207000
197000
187000
1
100
10000
Decay time (µs)
B)
Population Intensity
1
0.9
0.8
0.7
0.6
0.5
0.4
0.3
0.2
0.1
0
0
1
100
Rh (nm)

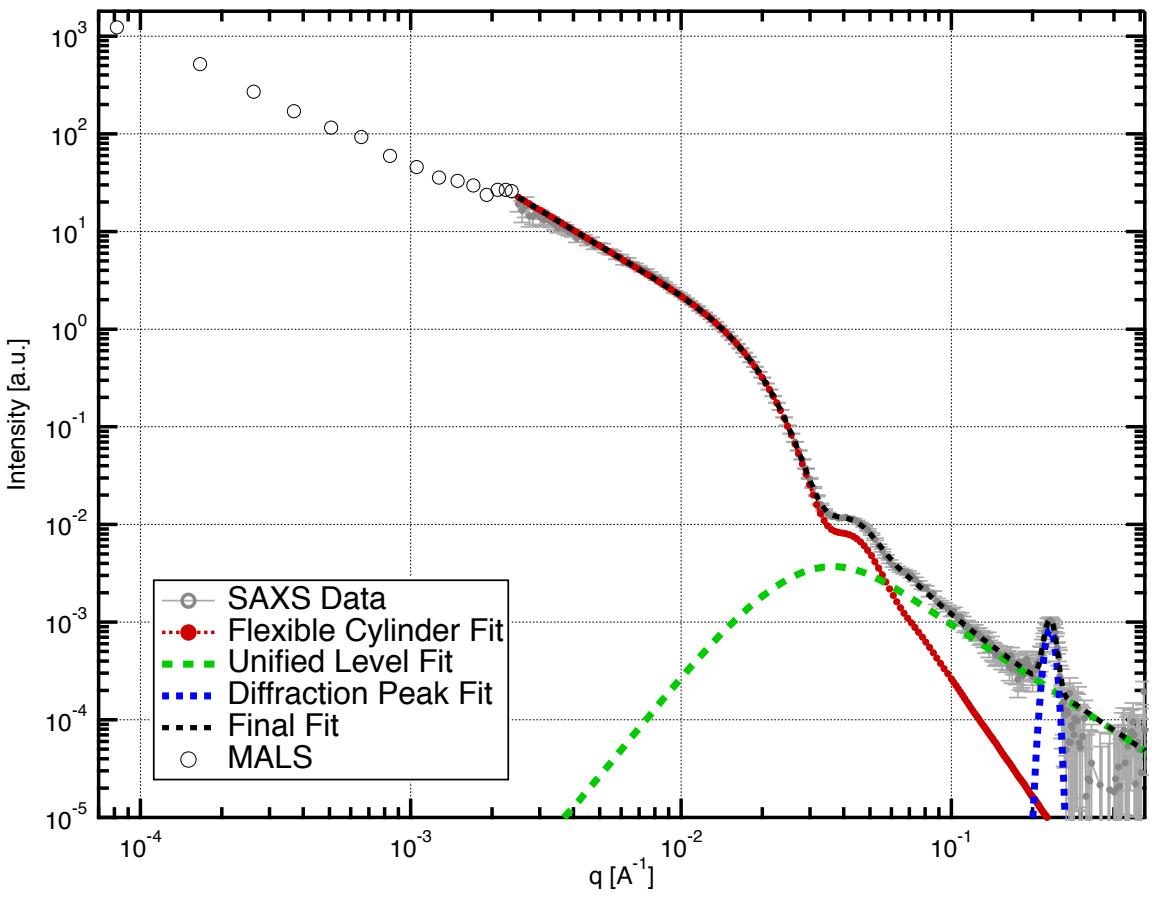
Intensity [a.u.]
q [A^{-1}]
SAXS Data
Flexible Cylinder Fit
Unified Level Fit
Diffraction Peak Fit
Final Fit
MALS

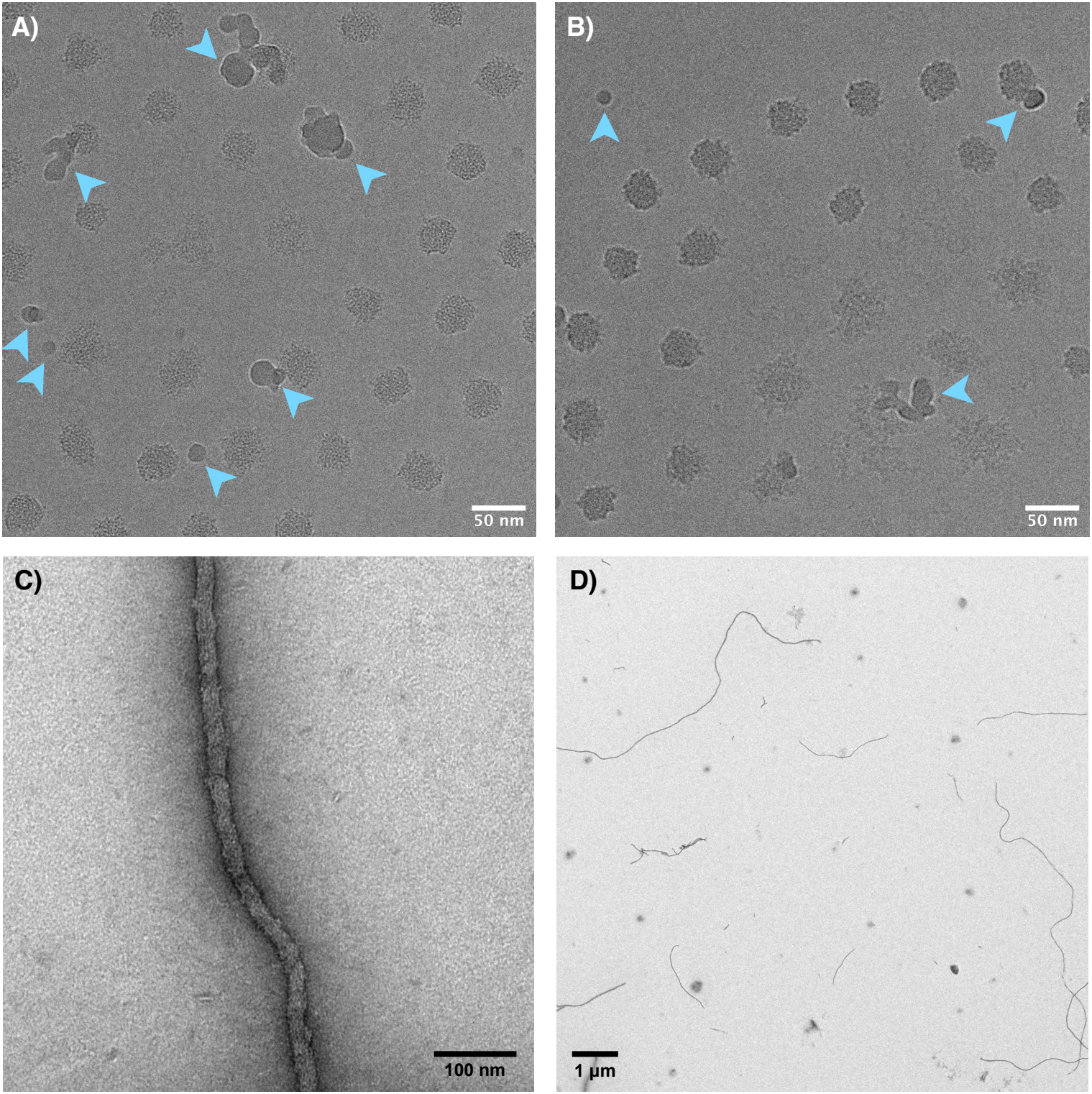
A)
50 nm
B)
50 nm
C)
100 nm
D)
1 µm

Name of Material/ Equipment	Company
70 mm circle filter paper	Whatman
Carbon Film TEM grid	Electron Microscopy Sciences
DAWN	Wyatt Technology
DNA oligonucleotide	Integrated DNA Nanotechnologies Inc
Lacey Carbon TEM grid	Electron Microscopy Sciences
Methoxy-poly(ethylene glycol)-block-poly(l-lysine hydrochloride) PEG5k - PLKC50	Alamanda Polymers Inc
Milli-Q	Millipore Sigma
NanoDrop	Thermo Scientific
negative-action tweezers	Dumont
Parafilm "M"	Bemis Company Inc
Quantifoil Holey Carbon TEM grid	Electron Microscopy Sciences
Research Goniometer and Laser Light Scattering System	Brookhaven Instruments
Slide-A-Lyzer G2 2K 0.5 mL	Thermo Scientific Pierce Protein Biology
small volume cuvette	Brookhaven Instruments
Solarus 950 Advanced Plasma System	Gatan
Talos TEM	FEI
Tecnai Spirit TEM	FEI
Uranyl Formate	SPI-Chem
Vitrobot	FEI

Catalog Number	Comments/Description
1001-070	Filter paper for wicking during grid prep
CF200-Cu	TEM grid
DAWN	MALS instrument
	Custom oligonucleotide
LC200-Cu	TEM grid
mPEG5K-b-PLKC50	Example block copolymer
	Ultrapure water
	For measuring nucleic acid concentration
N7	Tweezers for grid preparation
PM996	Laboratory film
Q210CR1.3	TEM grid
BI-200SM	DLS/MALS instrument
87723	Dialysis cartridge
BI-SVC	Cuvette for DLS/MALS
Solarus 950	Plasma system for TEM grids
Talos	TEM used for cryo samples
Spirit	TEM used for dry samples
16984-59-1	For negative staining samples for TEM
Vitrobot	Vitrification robot for cryo grid preparation

Response to reviewer comments

Reviewer 1:

The materials and results of this protocol are interesting and of high quality. The step-by-step instructions are mostly clear.

We thank the reviewer for their careful review of the manuscript, and for their time. Responses to specific comments follow.

I have the following comments:

1. What is meant by "slow dialysis"? Is there a way the dialysis can be performed too quickly?
We believe this comment refers to the salt annealing protocol described in the Introduction (lines 89 of the revised version). We have expanded this description to make it more clear. 'Slow', in this context, means that the salt concentration is decreased slowly relative to the time required for complexes to form and equilibrate at the maximum concentration where phase separation occurs. In the protocol, we explain the process by 1) stepping from 1M NaCl to 0.5M NaCl via dialysis over 24 hr, then two more days in dialysis to bring the buffer down to 1x PBS and 2) using low MWCO dialysis, both to ensure buffer exchange is slow. This is discussed more completely and compared to other assembly protocols in the referenced articles, but the protocol described here has worked well in our hands for several polymer pairs over a large range of lengths.

2. For Polymer Selection. What is the recommended range of number of charges for the charged blocks? A minimum is given. Is there a maximum?
Thank you for this question. We have not observed an upper limit. As noted in the manuscript, PCM size is determined by polymer block length, so the preferred block size will be application-specific. We have revised the manuscript to clarify both these points, and also added sample data in a new figure (Figure 2).

3. Similarly, could you be more specific about what the "rules" are for selecting PEG lengths.
Selection criteria are described in the same paragraph (Polymer Selection) referred to in the previous question. We state that a minimum neutral length is required for PCM formation, which increases with the length of the charged block, and include specific values for the case of pLys-PEG. Above this length, PCM corona size increases with neutral block length.

4. In PCM Assembly Preparation. An unknown amount of water in samples will complicate the calculations you have outlined. Is there drying step or are the materials supplied with an acceptable level of dryness?
Thank you for pointing this out. In our experience, commercial polymers and oligonucleotides are generally supplied with very low water content. This may not be the case for lab-synthesized polymers, and we have revised the manuscript to note this (line 135).

5. Preparation of Materials. Step 4.4 the pH is adjusted with NaOH or HCl. Does this provide a stable pH? Users might expect to use a buffer here.

6. 5.1.2 Define 10x PBS

The polymers are not resuspended in buffered solution, but the complexes are prepared with buffer, PBS (now defined in the manuscript, step 2.1.2) in this protocol. In principle, the individual polymer solutions could also be buffered, but this would require preparing different solutions for each final PCM buffer and also complicate the calculations. We added a recommendation to recheck the pH if solutions are stored for a long time.

7. 5.6.4. I would say "prepare dialysis solutions" since you are using fresh solutions for dialysis two more times.

Thank you. Changed as suggested.

8. 5.6.4.2 Dialysis is in 0.5M NaCl. Why not 0.15M NaCl which is closer to physiological? 1XPBS is saline which is supposed to be physiological.

The anneal does end in 1x PBS for exactly the reason you mention, but going right to 1x PBS would lead to significant swelling of the dialysis cartridges from the large difference in osmotic pressure, and also produce a faster initial change in ionic strength than the step dialysis protocol described here.

9. Do you recommend adding a preservative?

We have not found one to be necessary under typical laboratory conditions, but users could add one if it were necessary for their application. The choice of which to use would depend on that application, so we do not recommend one here.

10. For light scattering. I would state the filters and pore size used and why not filter the actual samples?

Thank you for this comment. We added information on the filters (step 3.1). Filtering nanoparticle solutions is a somewhat controversial topic, as it produces shear stress that can affect the morphology of the particles. Our opinion is that, if the constituent solutions are filtered carefully and the polymers are dissolved well, further filtration is not necessary, but we have not carried out careful studies of the effects of filtration and therefore are reluctant to state a recommendation.

11. Line 285. I am not sure what light scattering adds. You get all the useful information from SAXS.

Thank you for raising this point. One of the main hopes for this manuscript is to address the question of which characterization methods to use. Our experience is that SAXS, TEM, and static (MALS) or dynamic light scattering are in fact complementary, as they measure different, but overlapping aspects of the nanoparticle and that using more than one can dramatically increase confidence of the resulting characterization. We have expanded this section in the introduction and have moved some portions of the discussion here as well to make this more clear for the reader.

12. Line 304. PCMs lacking heavy atoms. Can you be specific about what is heavy?
As noted in the manuscript, the phosphorus in the DNA is the dominant contribution to the polymer scattering of pLys-PEG + DNA PCMs due to its higher electron density than the H/C/N/O atoms in the rest of the polymers. This can be estimated for any material, and we added a reference to do so in section 5.1.1.

Reviewer #2:

With interest I have read the manuscript on Assembly and characterization of polyelectrolyte complex micelles, by Tirrell et al.

I believe that the authors are really brave to make a short movie about PCMs and the characterization methods, however at present in my opinion a better focus is required.

I suggest to focus on PCMs filled with either DNA or RNA and only discuss the micellar structures so no worms, although these are interesting, you want the message to come through. If worms and other types of aggregates are included, it is difficult to follow the story.

We thank the reviewer for their suggestions and their time. In re-reading the manuscript, we agree that there are several aspects that can be made more clear, and we have attempted to do so in our revisions, while still maintaining the manuscript's focus on methodology. We have included more information on the strengths and complementarity of the various characterization methods, and also revised the section on polymer selection in response to both reviewers' comments, including adding a new figure (Figure 2) to illustrate the relationship between charged block length and PCM core size. We have also revised the opening paragraphs of the introduction to more clearly distinguish between PCMs in general and nucleic acid PCMs specifically, and we hope this addresses the concerns raised by the reviewer. One item about which there does seem to be some confusion is micelle shape; it appears to us that the reviewer is suggesting that micelles must be spherical, which conflicts with the standard usage of the term, e.g. packing parameter describing the shape of surfactant micelles. In the case of nucleic acid micelles, the shape (spheroids vs cylinders) is determined by the hybridization state of the nucleic acid, and we feel this is an important point to discuss, both as an interesting example of complexation physics and also because of its clear therapeutic relevance. Specific comments are addressed below.

* In the first paragraph of the introduction you explain PCMs in general, then a general picture of a PCM would be required as figure 1, with a homo polyanion. In figure 1 you specifically show PCMs with nucleic acids, which is fine if you focus on these.
Thank you for this suggestion. We have altered Figure 1 as suggested and have also revised the opening paragraphs as described above.

* In the abstract it is mentioned that you will discuss criteria for choosing polymers. This is very general, there are numerous examples of diblock copolymers and homopolymers which could

together form PCMs. Since you want to show that PCMs can be used to encapsulate nucleic acids, you already narrow down your system to DNA or RNA and cationic-neutral diblock copolymers.
We have revised Figure 1 as described above and revised the Polymer Selection section to explain what block length trends we have found when using nucleic acid polyanions.

* If you discuss the criteria I would expect a table or another kind of overview where the relationship between the length of the neutral block and the kind of structure you will get. Long blocks, small cores, due to steric pressure of the neutral blocks in the corona of the micelle, short blocks worms? Probably there is a relationship between the number of bases of nucleic acid and the length of neutral block needed to encapsulate it? I guess you can use the block length to tune the amount of material in the core?
Thank you for raising this question; we agree that we should have been more explicit in describing PCM structure-property relationships. We have added a new figure showing the relationship between core size and charged block length for pLys-PEG (Figure 2) and have made the relationship between nucleic acid hybridization and PCM shape more explicit.

* If you don't have worms, do you need MALS? Is your SAXS curve going up at high q? What is scattering at these length scales? Your TEM images show spherical objects with a diameter of ~30 nm and no bigger structures are seen. Which would correspond to the fitted core size of the particles ~22 nm.
* Additionally you fit the SAXS-curve with a combined form factor which contains "flexible cylinders", why do you need this for the micelles? You have spherical objects looking at your TEM images.
As the reviewer notes, spherical micelles should have flat scattering intensity at length scales larger than their diameter, and this is indeed what we observe (refs 7, 26). However, the data in question (Figures 4, 5c,d) are for cylindrical micelles which have lengths much larger than can be resolved by SAXS, are fit well by flexible cylinder models, and for which light scattering provides valuable information. We have revised the figure captions and discussion to make this more clear.

* In your manuscript I could only find the hydrodynamic radius mentioned in the caption of figure 1. It would be very useful to explain what is measured with which technique: DLS hydrodynamic radius, SAXS and TEM core size. The contrast between the chains in the corona and the solvent is too low to measure with SAXS and TEM. Also you mention the fitted core radius, but only show the size distribution histogram, it might be good to mention the hydrodynamic radius somewhere.
Thank you for this suggestion; we have revised the caption in question. As noted above, we have also revised the discussion of this topic and moved more of it to the introduction to emphasize the relative strengths and complementarity of the various techniques.

* About your SAXS measurements, most beamlines at synchrotrons can measure in absolute units. This means that you can estimate the mass and thus the aggregation number of your micelles from the intensity at q=0. This would be very useful, because it will give you an

estimate of the amount of nucleic acids which are present in the core of the micelles.
Thank you for this suggestion. We have added it to the discussion of SAXS in the introduction.

Other points:

* In PCM assembly it is explained how to calculate stoichiometric charge conditions, how did you take into account that polylysine is not fully charged at pH 7.4? If this polymers was forming a micelle with a weak polyanion I agree that both polymers would be fully charged, because of charge regulation. With strongly charged nucleic acids I am worried this is not the case.
Potentiometric titration of polylysine (see, for example, Ciferri et al, Biopolymers 6, 1019 (1968)) gives pKa values of roughly 10.2 – 10.3 for our salt concentrations at 25 deg C. While this is slightly depressed from the monomer value, it is still nearly three pH units above our working pH, so the approximation of being fully charged should be quite accurate for preparing the polycation solution. The question of charge distributions within the PCM core is a fascinating one, but also is not well understood and is, we believe, beyond the scope of this work.

* DLS: REPES software, where can I find it, I am familiar with CONTIN, which you can easily google, but I was not able to find the REPES software. Is it different from CONTIN?
REPES is an alternative approach to inverting Laplace transforms, so conceptually similar to CONTIN but handling noise a bit differently. The paper referenced in the manuscript contains a more complete description. We have added a subsection (3.7.2) discussing algorithm choice including CONTIN.

* For your SAXS experiments you use a buffer containing glycerol, is this to prevent radiation damage? If so it would be good to mention this and that people have to be careful with radiation damage of your samples, when using X-ray techniques.
Thank you for this suggestion. The glycerol is there as a radioprotectant, and we have amended the manuscript to explicitly note this (step 5.1.2). We discuss several methods to minimize radiation damage, including choice of flow cell vs capillary, exposure time and pattern, and online data analysis to detect damage.